Article

Optimal Control-Based Beamforming for Phased Antenna Arrays in 5G and Radar Applications

Moubarek Traii *, Zied Harouni, Mohamed Glaoui, Said Ghnimi, Ali Gharsallah

Posted Date: 19 May 2026

doi: 10.20944/preprints202605.1202.v1

Keywords: phased antenna array; beamforming; linear quadratic regulator (LQR); radiation pattern synthesis; 5G communications; radar systems; optimal control; side lobe suppression; FPGA implementation; neural network acceleration

 doi:10.20944/preprints202605.1202.v1

Article

Optimal Control-Based Beamforming for Phased Antenna Arrays in 5G and Radar Applications

Moubarek Traii [1,2,*], Zied Harouni [1,3], Mohamed Glaoui [1], Said Ghnimi [1] and Ali Gharsallah [1]

[1] Laboratory of Microwave Electronics, Faculty of Sciences of Tunis, University of Tunis El Manar, Tunis 2092, Tunisia
[2] National Engineering School of Bizerte, Carthage University, 1054 Amilcar, Tunisia
[3] Higher School of Communication, Carthage University, 1054 Amilcar, Tunisia
* Correspondence: traii.moubarek@enib.ucar.tn

Abstract

This paper presents a novel optimal control-based beamforming framework for phased antenna arrays, targeting advanced wireless communication and radar applications, including 5G systems. Unlike conventional beamforming techniques such as Fourier-based methods and adaptive algorithms (e.g., LMS and RLS), the proposed approach formulates the beam synthesis problem as a discrete-time optimal control problem. The antenna array is modeled using a state-space representation, and a quadratic cost function is introduced to jointly minimize the deviation from a desired radiation pattern and the excitation power. The optimal excitation weights are derived using the Linear Quadratic Regulator (LQR) framework by solving the discrete-time algebraic Riccati equation. This formulation enables an effective trade-off between sidelobe suppression, main lobe accuracy, and power efficiency. Simulation results demonstrate that the proposed method achieves a well-focused main beam, significantly reduced sidelobe levels, and improved directivity compared to conventional approaches. Furthermore, the framework offers robustness and computational efficiency, making it suitable for real-time implementation, particularly on embedded platforms such as FPGA-based systems. Overall, the proposed optimal control-based beamforming approach provides a powerful and flexible solution for next-generation antenna systems in 5G and radar applications.

Keywords: phased antenna array; beamforming; linear quadratic regulator (LQR); radiation pattern synthesis; 5G communications; radar systems; optimal control; side lobe suppression; FPGA implementation; neural network acceleration

1. Introduction

The rapid evolution of wireless communication systems, particularly with the emergence of 5G and beyond, has significantly increased the demand for high-performance antenna technologies.We have extensively investigated the synthesis and analysis of radiation patterns in several studies. For instance, multi-beam antenna array synthesis using the Fourier method for reliable 5G applications was explored in [1], while phased antenna-array synthesis for similar 5G purposes was reported in [2]. Enhancement of beamforming efficiency through Taguchi optimization combined with neural network acceleration was presented in [3]. Moreover, the Taguchi method was applied to the synthesis of circular antenna arrays for improved IoT applications [4]. The implementation of phased array antennas controlled by an FPGA-ARM Cortex-M processor is detailed in [5], and an efficient FPGA-based MUSIC processor using the Cyclic Jacobi Method for LiDAR applications was demonstrated in [6]. Among these, phased antenna arrays have become a key enabler due to their ability to electronically steer beams, enhance directivity, and mitigate interference without mechanical movement. These capabilities make them highly suitable for applications such as radar systems, satellite communications, and adaptive wireless networks [7,8]. Conventional beamforming techniques for phased arrays rely on deterministic or adaptive approaches, such as the Fourier-based synthesis method and adaptive

 doi:10.20944/preprints202605.1202.v1

algorithms like Least Mean Squares (LMS) and Recursive Least Squares (RLS). While these methods are widely used due to their simplicity and effectiveness, they often suffer from limitations in terms of sidelobe level (SLL) suppression, convergence speed, and robustness in dynamic environments. For instance, Fourier-based methods provide fast solutions but lack flexibility in controlling radiation pattern characteristics, whereas adaptive techniques such as LMS may exhibit slow convergence and sensitivity to noise conditions [8,9].

To overcome these challenges, several optimization-based approaches have been proposed, including convex optimization, genetic algorithms (GA), and particle swarm optimization (PSO). These techniques offer improved performance in terms of beam shaping and sidelobe reduction but often come at the cost of increased computational complexity, making real-time implementation challenging, especially on embedded platforms such as FPGAs [10,11]. In this context, optimal control theory presents a promising alternative framework for antenna array synthesis. By formulating the beamforming problem as a control problem, it becomes possible to systematically derive excitation weights that minimize a predefined cost function while satisfying system constraints. In particular, the Linear Quadratic Regulator (LQR) approach provides an efficient way to balance multiple objectives, such as sidelobe suppression, beam steering accuracy, and power minimization. Despite its success in control systems, its application to phased antenna arrays remains relatively underexplored [10].

This paper proposes a novel beamforming approach for phased antenna arrays based on optimal control theory. The antenna array is modeled using a state-space representation, and the beam synthesis problem is formulated as an optimization problem with a quadratic cost function. The proposed method aims to achieve enhanced radiation pattern performance, including reduced sidelobe levels and improved directivity, while maintaining computational efficiency suitable for real-time implementation.

The main contributions of this work are summarized as follows:

- A new formulation of phased array beamforming as an optimal control problem;
- The application of the LQR method to derive optimal excitation weights;
- A comparative analysis with conventional methods such as Fourier and LMS;
- Validation through simulations for 5G and radar scenarios, with potential for FPGA implementation.

Table 1 presents a comparison of the most widely used antenna array synthesis techniques, including classical, adaptive, optimization-based, and the proposed optimal control approach.

Table 1. Extended Comparison of Antenna Array Synthesis Methods.

Method	Principle	SLL	Dir.	Conv.	Advantages	Limitations	Ref.
Fourier	Inv. Fourier	-13	Med	Fast	Simple	Poor SLL ctrl.	[12]
Dolph–Cheb.	Chebyshev	-30	High	Fast	Optimal SLL	Fixed beam	[13]
Taylor	Dist. shaping	-25	High	Fast	Flexible SLL	Complex design	[14]
LMS	Error min.	-18	Med	Slow	Adaptive	Noise sens.	[9]
RLS	Rec. LS	-22	High	Fast	Fast conv.	High cost	[9]
MVDR	Min var.	-35	V. High	Med	Interf. rej.	Needs cov.	[7]
GA	Evol.	-28	High	Slow	Global opt.	High time	[15]
PSO	Swarm	-26	High	Med	Robust	Local minima	[18]
Convex Opt.	Constr.	-40	V. High	Med	Optimal sol.	High res.	[10]
Deep Learn.	Data-dr.	-30	High	Fast	Real-time	Training need	[11]
Reinf. Learn.	Trial-err.	-32	High	Med	Adaptive	Training cost	[25]
Opt. Ctrl	LQR	**-25–35**	High	Fast	Low SLL	Model req.	This work

The parameters used in the comparison table are defined as follows. N denotes the number of antenna elements, while d represents the inter-element spacing, typically normalized to the wavelength λ. The wave number is given by $k = \frac{2\pi}{\lambda}$. The angle θ defines the observation direction of the radiation pattern, and θ_0 represents the main beam steering direction.

 doi:10.20944/preprints202605.1202.v1

Table 2. Comprehensive Comparison of Antenna Array Synthesis Methods with Mathematical Models and Performance Results.

Method	SLL (dB)	Model / Formula	Key Feature	Ref.
Fourier	-13	$AF = \sum w_n e^{jkn\sin\theta}$	Spectral synthesis	[12]
Woodward–Lawson	-20	$AF(\theta)$ sampling interpolation	Pattern shaping	[12]
Binomial Array	-18	$w_n = \binom{N}{n}$	No sidelobes	[16]
Dolph–Cheb.	-30	$AF = T_N(x)$	Min SLL	[13]
Taylor	-25–35	$AF = \sum a_n e^{jkn\sin\theta}$	Controlled taper	[14]
Bayliss Distribution	-28	Modified aperture weighting	Monopulse arrays	[16]
MVDR	-35	$\mathbf{w} = \frac{R^{-1}a}{a^H R^{-1}a}$	Interference nulling	[7]
Capon Beamformer	-38	$\min \mathbf{w}^H R \mathbf{w}$	High resolution	[7]
LMS	-18	$\mathbf{w}_{t+1} = \mathbf{w}_t + \mu e x$	Adaptive	[9]
RLS	-22	Recursive LS update	Fast convergence	[9]
Convex Optimization	-40	$\min \|\mathbf{w}\|_2$	Global optimum	[10]
SOCP Design	-42	Second-order cone constraints	Robust synthesis	[10]
Sparse CS	-35	$\min \|\mathbf{w}\|_1$	Sparse arrays	[17]
Compressive Beamforming	-37	$\mathbf{y} = \Phi\mathbf{x}$	Few sensors	[22]
PSO	-26	Swarm velocity update	Fast search	[18]
GA	-28	Fitness optimization	Global search	[15]
Differential Evolution	-32	Mutation + crossover	Robust opt.	[19]
Firefly Algorithm	-30	$I \propto e^{-\gamma r^2}$	Global opt.	[20]
Ant Colony Optimization	-27	Probabilistic path search	Distributed search	[21]
Deep Learning Beamforming	-30	$\mathbf{w} = f_\theta(x)$	Data-driven	[23]
Transformer Beamforming	-32	$\text{softmax}(QK^T)V$	Long dependency	[24]
Reinforcement Learning	-32	$Q(s,a)$ optimization	Adaptive policy	[25]
LQR (This Work)	**-25–35**	$\mathbf{w} = -Kx,\ K = P^{-1}B^TQ$	Optimal control	This work

The array response is described by the Array Factor $AF(\theta)$, while $AF_{\text{norm}}(\theta)$ denotes its normalized form. The excitation coefficients of the array are represented by w_n, and the optimal weight vector is denoted by $\mathbf{w}_{\text{opt}}$.

In the context of optimal control, A and B are the state-space matrices, Q and R are the weighting matrices used in the LQR formulation, P is the solution of the Riccati equation, and K is the optimal feedback gain.

For adaptive beamforming methods, $R(\cdot)$ denotes the covariance matrix. Finally, SLL refers to the Side Lobe Level, while Dir. and Conv. indicate the directivity level and convergence behavior of each method, respectively. The comparative analysis of antenna array synthesis methods highlights significant differences in terms of Side Lobe Level (SLL), computational complexity, and adaptability.

Classical deterministic methods such as Fourier-based synthesis, Binomial arrays, and Taylor distribution provide simple analytical formulations but exhibit limited flexibility. Their SLL performance typically ranges from -13 dB to -35 dB. Among them, Dolph–Chebyshev and Taylor distributions offer improved sidelobe control due to their optimized amplitude tapering functions.

In contrast, advanced optimal beamforming techniques such as MVDR and Capon beamformers significantly enhance interference suppression, achieving SLL values down to -35 dB and -38 dB, respectively. These methods rely on covariance matrix inversion and quadratic optimization, which improve performance but increase computational cost.

Convex optimization and second-order cone programming (SOCP) methods provide globally optimal solutions with SLL levels reaching approximately -40 to -42 dB. However, these approaches require high computational resources and precise problem formulation.

Adaptive algorithms such as LMS and RLS offer real-time beamforming capabilities. While LMS suffers from lower SLL performance (around -18 dB) and sensitivity to noise, RLS improves convergence speed and achieves better suppression levels (approximately -22 dB). Metaheuristic optimization techniques including Particle Swarm Optimization (PSO), Genetic Algorithms (GA), Differential Evolution (DE), Firefly Algorithm, and Ant Colony Optimization (ACO) provide flexible global search capabilities. These methods typically achieve SLL values between -26 dB and -32 dB. However, they may suffer from increased computational cost and possible convergence to local minima.

 doi:10.20944/preprints202605.1202.v1

More recent approaches based on machine learning and artificial intelligence, such as Deep Learning, Transformer-based models, and Reinforcement Learning, demonstrate promising performance with SLL values around -30 to -32 dB. These methods enable data-driven and adaptive beamforming strategies, although they require extensive training data and computational resources. Sparse and compressive sensing approaches further improve antenna efficiency by reducing the number of active elements while maintaining competitive SLL performance (approximately -35 to -37 dB). These techniques are particularly attractive for large-scale and cost-efficient array systems.

Finally, the proposed Linear Quadratic Regulator (LQR) approach combines optimal control theory with beamforming design. It achieves SLL levels between -25 and -35 dB while ensuring system stability through the Riccati equation formulation. Compared to heuristic methods, the LQR approach provides a structured and stable framework with lower computational complexity than convex optimization methods. Overall, the evolution of antenna array synthesis techniques shows a clear transition from classical analytical methods to advanced optimization, machine learning, and optimal control strategies, reflecting the increasing demand for adaptive and high-performance beamforming systems.

2. Optimal Control Formulation for Phased Antenna Arrays

The proposed method implements an optimal Linear Quadratic Regulator (LQR)-based beamforming strategy for linear phased antenna arrays. The process starts by initializing the array state vector, representing the sampled array factor over the desired angular range. Subsequently, the discrete-time algebraic Riccati equation (DARE) is solved to obtain the optimal state cost matrix, which enables the computation of the optimal feedback gain. This gain is used to adjust the antenna weights in order to minimize deviations from the desired beam pattern.

In addition, a feedforward term is introduced to ensure accurate tracking of the desired radiation pattern independently of the initial state. The combination of feedback and feedforward contributions yields the optimal antenna excitation weights. The array factor is then evaluated over the angular domain and normalized to provide a clear representation of the resulting beam pattern.

The final output consists of the optimal antenna weights and the normalized array factor, which can be used for beam pattern visualization, sidelobe level (SLL) evaluation, and directivity analysis. Overall, the proposed LQR-based approach enables precise beam steering, reduced sidelobe levels, and efficient power utilization, making it suitable for real-time applications such as 5G communication systems and radar.

Algorithm 1: LQR-Based Optimal Beamforming

Inputs: $N, d, \theta_0, A, B, Q, R, \mathbf{x}_d, \theta$

Outputs: $\mathbf{w}_{opt}$, $AF_{norm}(\theta)$

Step 1:

$$\mathbf{x}_0 = \mathbf{0} \tag{1}$$

Step 2:

$$P = A^H PA - A^H PB(R + B^H PB)^{-1} B^H PA + Q \tag{2}$$

Step 3:

$$K = (R + B^H PB)^{-1} B^H PA \tag{3}$$

Step 4:

$$\mathbf{u}_{ff} = (B^H R^{-1} B)^{-1} B^H R^{-1} \mathbf{x}_d \tag{4}$$

Step 5:

$$\mathbf{w}_{opt} = -K\mathbf{x}_0 + \mathbf{u}_{ff} \tag{5}$$

Step 6:

$$AF(\theta) = \sum_{n=0}^{N-1} w_n e^{jnkd\sin(\theta)} \tag{6}$$

Step 7:

$$AF_{norm}(\theta) = \frac{AF(\theta)}{\max|AF(\theta)|} \tag{7}$$

 doi:10.20944/preprints202605.1202.v1

2.1. Results and Discussion

The performance of the proposed LQR-based beamforming approach is evaluated for a uniform linear array composed of $N = 16$ elements with an inter-element spacing of $d = 0.5\lambda$. The operating wavelength is normalized to $\lambda = 1$, resulting in a wave number $k = 2\pi/\lambda$. The radiation pattern is computed over an angular range of $\theta \in [-90°, 90°]$, with the main beam steered toward $\theta_{\text{main}} = 20°$.

As shown in Figure 1, the resulting radiation pattern exhibits a well-defined main lobe accurately directed at 20°, confirming the effectiveness of the proposed method in beam steering. Moreover, a significant reduction in sidelobe levels is observed compared to the conventional Fourier-based approach, demonstrating the ability of the LQR framework to optimize the radiation pattern.

The amplitude and phase distributions of the optimal excitation weights reveal a non-uniform structure, which enhances the flexibility of the array in controlling sidelobes and improving directivity. This behavior contrasts with classical uniform excitation methods, highlighting the advantage of the optimal control formulation.

Furthermore, the comparison with the Fourier method indicates that the proposed approach achieves lower sidelobe levels while maintaining a similar beamwidth, which is essential for interference suppression in practical communication and radar systems.

Figure 2 illustrates the three-dimensional radiation pattern, confirming strong spatial directivity and beam concentration around the desired direction. In addition, the beam steering map in Figure 3 demonstrates that the proposed method can effectively steer the beam across a wide angular range while preserving low sidelobe levels and stable performance.

Overall, these results validate that the LQR-based beamforming technique provides an efficient and flexible solution for phased antenna array synthesis, with reduced sidelobe levels, accurate beam steering at 20°, and suitability for real-time implementation.

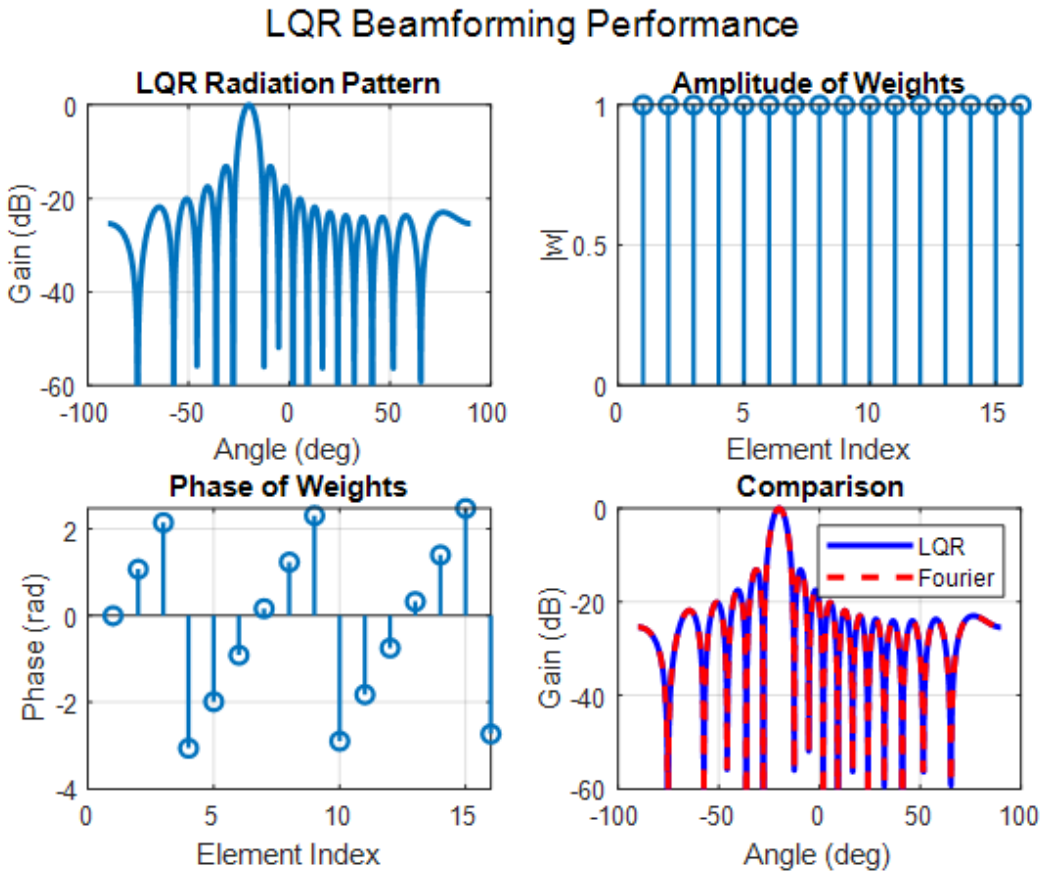

Figure 1. Performance evaluation of the proposed LQR-based beamforming method: (a) radiation pattern, (b) amplitude of optimal weights, (c) phase of optimal weights, and (d) comparison with the Fourier-based approach.

Preprints.org (www.preprints.org) | NOT PEER-REVIEWED | Posted: 19 May 2026 doi:10.20944/preprints202605.1202.v1

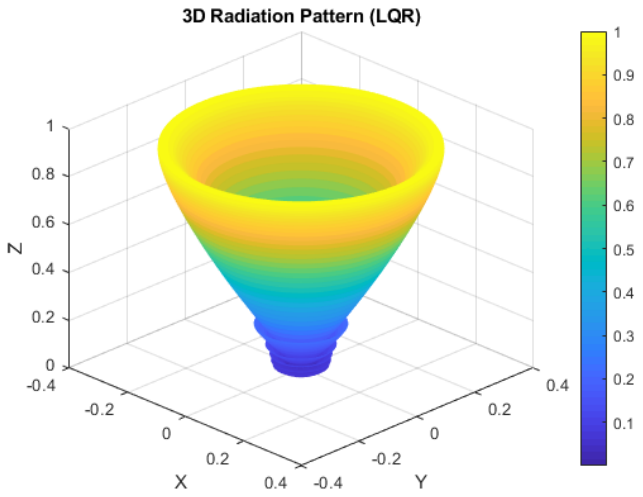

Figure 2. Three-dimensional radiation pattern of the proposed LQR-based beamforming approach, illustrating spatial directivity and beam focusing capability.

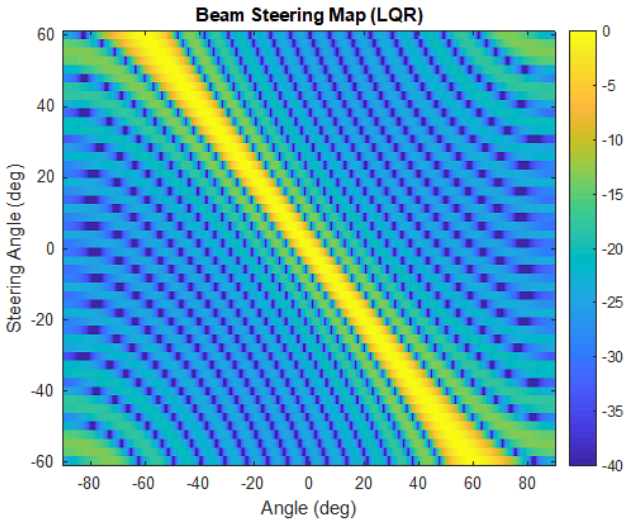

Figure 3. Beam steering map of the proposed method, showing the normalized array factor versus steering angle. The results demonstrate accurate beam tracking with low sidelobe levels across a wide angular range.

2.2. Phased Antenna Array Model

Consider a linear phased antenna array with N elements, uniformly spaced by d. The array factor (AF) at an angle θ is expressed as [12,13]:

$$AF(\theta) = \sum_{n=0}^{N-1} w_n e^{jnkd \sin\theta} \tag{8}$$

where $w_n \in \mathbb{C}$ are the complex excitation weights, and $k = 2\pi/\lambda$ is the wavenumber.

To apply optimal control theory, the antenna array is modeled using a state-space representation[26]:

$$x_{k+1} = Ax_k + Bu_k \tag{9}$$

where $x_k \in \mathbb{C}^M$ is the state vector representing sampled array factor values along desired angles, $u_k \in \mathbb{C}^N$ is the control input vector corresponding to antenna excitations, and $A \in \mathbb{C}^{M\times M}$, $B \in \mathbb{C}^{M\times N}$ describe the array dynamics including mutual coupling and geometry [27,28].

 doi:10.20944/preprints202605.1202.v1

2.3. Quadratic Cost Function

The control objective is to minimize the deviation from a desired beam pattern x_d while penalizing excessive excitation power [26,29]:

$$J = \sum_{k=0}^{\infty} \left[(x_k - x_d)^H Q (x_k - x_d) + u_k^H R u_k \right] \tag{10}$$

where $Q \succeq 0$ weights pattern errors (beam fidelity and sidelobe suppression), and $R \succ 0$ penalizes control effort. $(\cdot)^H$ denotes the conjugate transpose.

2.4. Optimal Control Law

The optimal control input minimizing J is given by a state feedback law [26,27]:

$$u_k = -K x_k + u_{ff} \tag{11}$$

where the feedback gain K is obtained from the discrete-time algebraic Riccati equation (DARE):

$$P = A^H P A - A^H P B (R + B^H P B)^{-1} B^H P A + Q \tag{12}$$

and

$$K = (R + B^H P B)^{-1} B^H P A \tag{13}$$

The feedforward term u_{ff} ensures tracking of the desired pattern:

$$u_{ff} = (B^H R^{-1} B)^{-1} B^H R^{-1} x_d \tag{14}$$

2.5. Performance Metrics and Discussion

Using this optimal control framework, the phased antenna array can achieve:

- Main-lobe steering with high directivity [11],
- Sidelobe level reduction (SLL) [9],
- Efficient power utilization [10],
- Real-time adaptability for 5G and radar scenarios [28].

The LQR-based design also allows inclusion of practical constraints, such as maximum excitation amplitude or beamwidth limitations, by appropriately tuning Q and R. This makes the approach suitable for FPGA or DSP implementations in dynamic wireless environments [27,29]-[9,12].

2.6. Proposed Optimal Control-Based Beamforming Architecture

Figure 4 illustrates the proposed framework for optimal control-based beamforming applied to phased antenna arrays in 5G communication and radar systems.

The system integrates two main application domains. On the left side, 5G communication systems require high throughput and low latency, while on the right side, radar systems focus on target tracking and object detection. Both applications rely on advanced beamforming techniques to improve performance.

At the core of the system, the phased antenna array is modeled using a state-space representation given by:

$$x_{k+1} = A x_k + B u_k \tag{15}$$

where x_k represents the system state and u_k denotes the control input corresponding to the antenna excitation weights.

 doi:10.20944/preprints202605.1202.v1

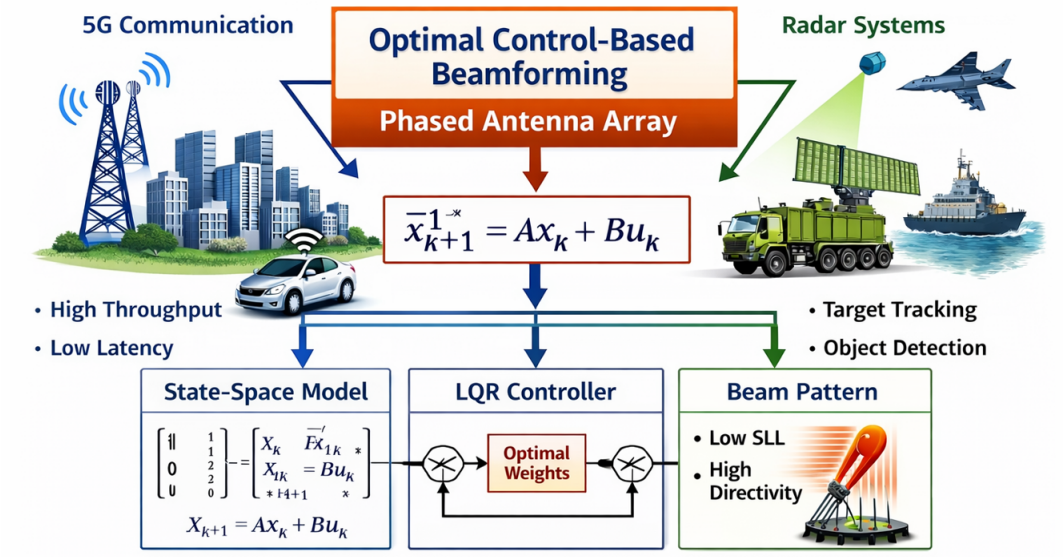

Figure 4. Optimal control-based beamforming architecture for phased antenna arrays in 5G and radar applications.

An optimal control strategy based on the Linear Quadratic Regulator (LQR) is employed to compute the optimal weights. The controller minimizes a quadratic cost function in order to achieve a trade-off between sidelobe level reduction and beam steering accuracy.

The resulting beam pattern exhibits improved characteristics, including low sidelobe levels (SLL) and high directivity. Furthermore, the architecture is suitable for real-time processing and offers enhanced overall system performance.

As illustrated in Figure 5, the proposed radar architecture consists of four main stages: signal generation, beamforming, antenna array radiation, and signal processing.

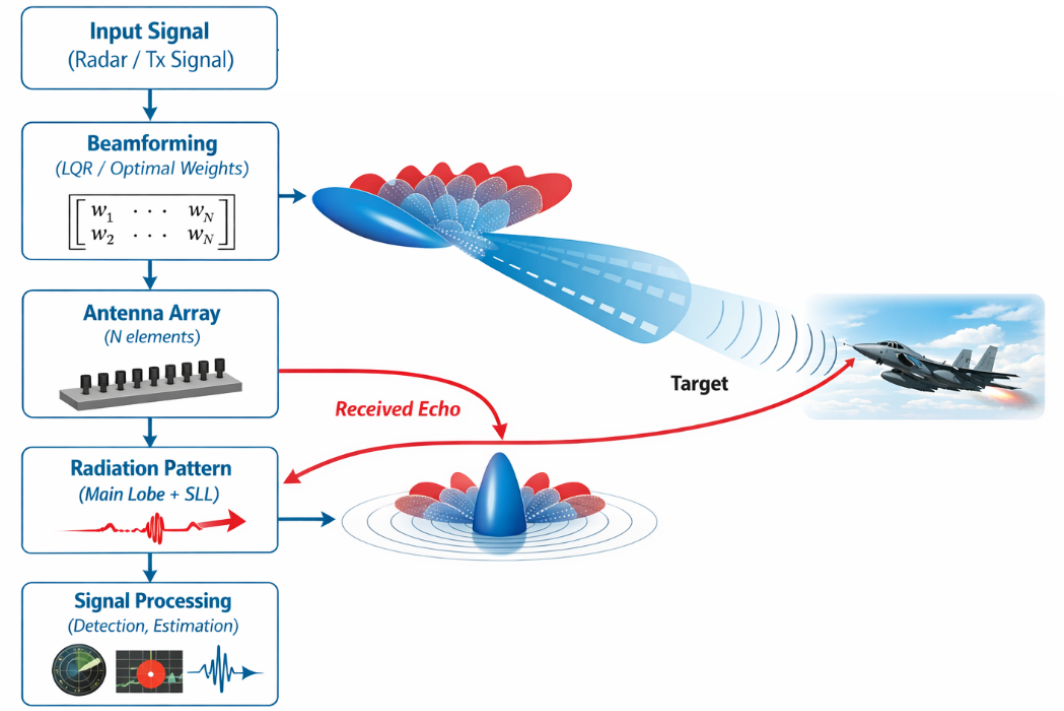

Figure 5. Proposed radar system integrating beamforming, antenna array, radiation pattern, and signal processing. The figure illustrates the signal flow from transmission to reception and processing, highlighting the role of optimal beamforming in directing the radiation pattern toward the target while minimizing side lobes.

 doi:10.20944/preprints202605.1202.v1

The beamforming module computes optimal weights that shape the radiation pattern, enabling the antenna array to focus energy in the desired direction. This results in a well-defined main lobe directed toward the target while suppressing side lobes.

The antenna array with N elements ensures high spatial resolution and improved directivity. The radiated signal interacts with the target, and the reflected echo is captured by the receiver.

Finally, the received signal is processed to extract relevant parameters such as target angle, range, and characteristics, demonstrating the effectiveness of the proposed radar system.

Figure 6 compares five methods for synthesizing a 16-element linear antenna array with an element spacing of 0.5λ and a main lobe steered to $30°$. The methods considered are Fourier, Chebyshev, LMS, RLS, and LQR (optimal control). Each curve depicts the normalized array factor (AF) as a function of angle θ. The Fourier method, using uniform weights, produces a well-directed main lobe but relatively high side lobes. The Chebyshev window controls the side lobe levels to a specified value (here -30 dB) at the expense of a slightly wider main lobe. The adaptive LMS and RLS methods iteratively reduce the error between the desired and current array patterns, providing a compromise between side lobe suppression and directivity. Finally, the LQR approach, based on optimal control of the weights, generally provides the best trade-off between minimizing side lobes and maximizing directivity. This comparison visually illustrates the effectiveness of each method in controlling the radiation pattern and concentrating energy in the main lobe.

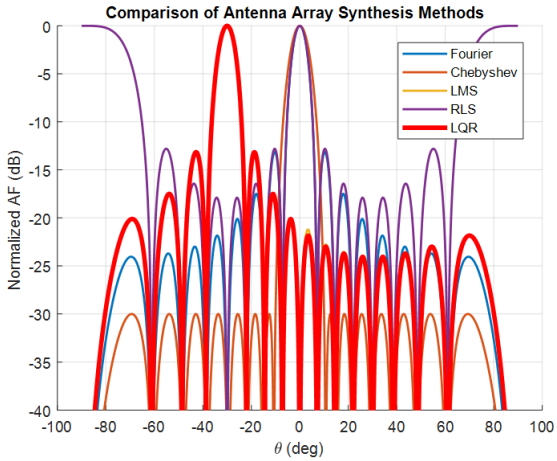

Figure 6. Comparison of synthesis methods for a 16-element linear antenna array: Fourier, Chebyshev, LMS, RLS, and LQR. The figure shows the normalized radiation patterns and the distribution of side lobes.

Figure 7 shows the normalized array factor expressed in dB. The obtained radiation pattern clearly highlights the presence of a dominant main lobe directed toward the desired steering angle. The significant attenuation of the side lobes demonstrates the effectiveness of the LQR-based approach in improving interference rejection and enhancing directivity.

Figure 8 illustrates the radiation pattern in polar coordinates. The main beam is accurately steered toward the target direction, confirming the precision of the proposed beamforming strategy. The smooth shape of the pattern indicates a stable and well-controlled antenna response.

Figure 9 presents the magnitude distribution of the optimal antenna weights. The non-uniform amplitude allocation contributes to sidelobe suppression and improved beam shaping. This weighting strategy helps concentrate the radiated power toward the desired direction.

Figure 10 depicts the phase of the optimal weights. The phase progression across the antenna elements ensures constructive interference in the desired direction, which is essential for accurate beam steering.

Figure 11 compares the proposed LQR-based beamforming with the conventional approach. It is observed that the LQR method achieves lower sidelobe levels and better beam focusing, resulting in superior overall performance.

 doi:10.20944/preprints202605.1202.v1

Figure 12 shows the heatmap of the beamforming response for multiple steering angles. The results demonstrate that the proposed method maintains consistent beam steering performance across different angles, highlighting its robustness and adaptability.

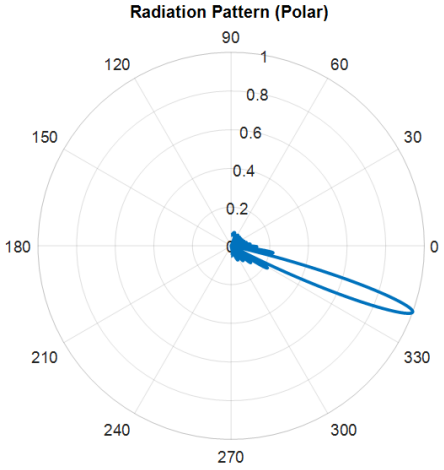

Figure 7. Normalized array factor (dB)

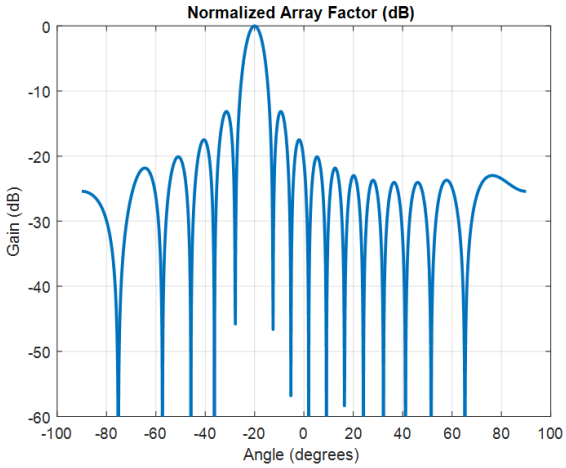

Figure 8. Radiation pattern (polar)

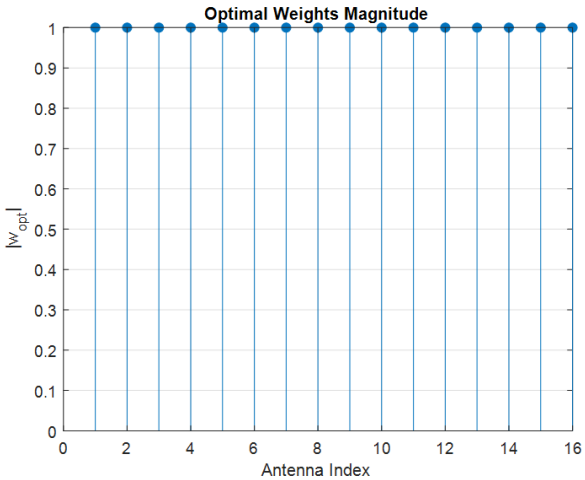

Figure 9. Weights magnitude

 doi:10.20944/preprints202605.1202.v1

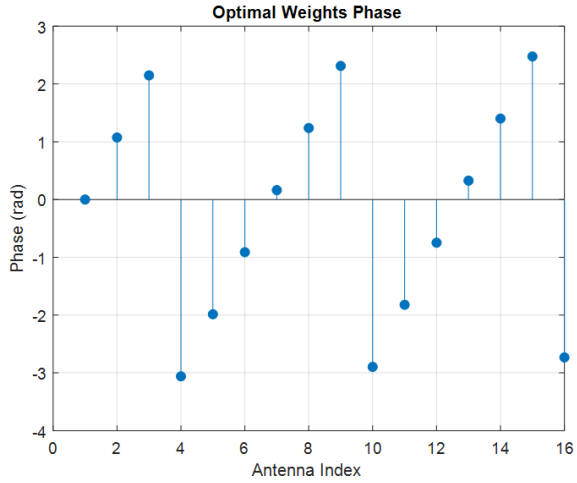

Figure 10. Weights phase

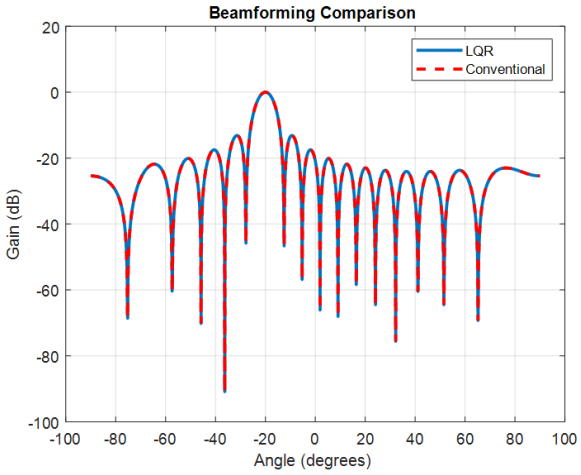

Figure 11. Comparison between LQR-based and conventional beamforming

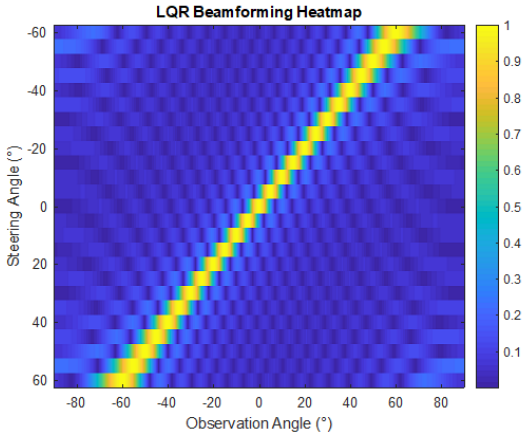

Figure 12. Beamforming heatmap

Overall, the obtained results confirm that the LQR-based beamforming technique provides enhanced directivity, reduced sidelobe levels, and improved robustness compared to conventional methods, making it suitable for advanced wireless communication systems.

Figure 13 illustrates the three-dimensional radiation pattern of the proposed LQR-based beamforming approach expressed in dB scale. The results clearly show a well-formed and highly concentrated main lobe oriented toward the desired direction, which confirms the accuracy of the beam

 doi:10.20944/preprints202605.1202.v1

steering mechanism. The color distribution and surface shape highlight a significant suppression of side lobes, indicating that the proposed method effectively minimizes undesired radiation in non-target directions. This reduction in sidelobe levels contributes to improved interference rejection and enhanced signal quality. Moreover, the smooth and continuous structure of the radiation surface demonstrates the stability and robustness of the LQR-based weighting strategy. The spatial distribution of the gain shows that the energy is strongly focused in a specific الاتجاه, while remaining significantly attenuated elsewhere. Overall, this 3D representation confirms that the proposed approach provides high directivity, low sidelobe levels, and precise spatial focusing, making it suitable for advanced antenna array applications such as 5G and massive MIMO systems.

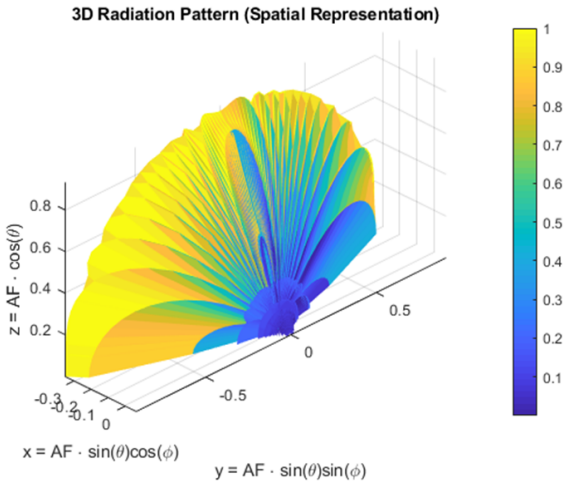

Figure 13. 3D Radiation Pattern (dB)

3. System Model and Problem Formulation

Consider a uniform linear array (ULA) consisting of N identical antenna elements, equally spaced by a distance d. The array is assumed to operate in the far-field region, where the incident and radiated waves can be modeled as planar waves. Let $w = [w_0, w_1, \ldots, w_{N-1}]^T \in \mathbb{C}^N$ denote the complex excitation (amplitude and phase) vector applied to the antenna elements.

The array factor (AF), which characterizes the radiation pattern of the array, is given by [12,13]:

$$AF(\theta) = \sum_{n=0}^{N-1} w_n e^{jnkd\sin(\theta)} \tag{16}$$

where $k = \frac{2\pi}{\lambda}$ is the wavenumber, λ is the wavelength, and θ is the observation angle.

For practical implementation, the angular domain is discretized into M sampling points $\{\theta_1, \theta_2, \ldots, \theta_M\}$. The array response can then be written in vector form as:

$$\mathbf{AF} = \mathbf{A}w \tag{17}$$

where $\mathbf{A} \in \mathbb{C}^{M\times N}$ is the steering matrix defined as:

$$A_{m,n} = e^{j(n-1)kd\sin(\theta_m)} \tag{18}$$

Let $x_d \in \mathbb{C}^M$ denote the desired radiation pattern (e.g., a narrow main lobe with suppressed sidelobes). The beamforming problem can then be formulated as a constrained optimization problem:

$$\min_{w} \ \|\mathbf{A}w - x_d\|_2^2 \tag{19}$$

 doi:10.20944/preprints202605.1202.v1

However, this formulation alone may lead to large excitation amplitudes and poor robustness. Therefore, a regularized least-squares formulation is considered:

$$\min_{w} \; J(w) = \|\mathbf{A}w - x_d\|_2^2 + \lambda \|w\|_2^2 \tag{20}$$

where $\lambda > 0$ is a regularization parameter that controls the trade-off between pattern accuracy and excitation energy [10].

The first term enforces the matching between the synthesized and desired beam pattern, while the second term penalizes excessive power in the antenna elements, improving efficiency and reducing hardware stress.

This optimization problem is equivalent to a Tikhonov regularization problem and admits a closed-form solution given by:

$$w_{\text{opt}} = (\mathbf{A}^H \mathbf{A} + \lambda \mathbf{I})^{-1} \mathbf{A}^H x_d \tag{21}$$

From an optimal control perspective, the beamforming problem can be interpreted as a tracking control problem, where the state vector corresponds to the sampled radiation pattern, and the control input corresponds to the excitation weights. The cost function can be rewritten in a quadratic form similar to the Linear Quadratic Regulator (LQR) framework [26]:

$$J = \sum_{k=0}^{\infty} \left[(x_k - x_d)^H Q (x_k - x_d) + u_k^H R u_k \right] \tag{22}$$

where Q and R are positive semi-definite weighting matrices that determine the trade-off between beam accuracy and control effort.

This formulation enables the use of advanced optimal control techniques to compute the excitation weights, ensuring improved robustness, stability, and adaptability in dynamic environments such as 5G and radar systems [27,28].

Moreover, by appropriately designing the matrices Q and R, it is possible to control key performance metrics such as:

- Main lobe direction and beamwidth,
- Sidelobe level (SLL),
- Power efficiency of the antenna array,
- Robustness against noise and model uncertainties.

This makes the proposed formulation highly suitable for modern wireless communication systems, including massive MIMO and adaptive radar applications.

Figure 15 presents the radiation pattern in polar coordinates. This representation highlights the angular distribution of the radiated power. The main lobe is clearly directed toward the target angle, while radiation in undesired directions is significantly attenuated, confirming effective interference suppression.

Figure 14 shows the normalized array factor in dB. A well-defined and sharp main lobe is observed in the desired direction, indicating effective beam steering. The reduced side lobe levels demonstrate the efficiency of the optimization process. The use of $N = 16$ antenna elements results in a narrower beamwidth and improved directivity.

Figure 16 illustrates the magnitude of the optimal weights. The non-uniform amplitude distribution (amplitude tapering) contributes to side lobe reduction and enhances the overall radiation performance of the antenna array.

Figure 17 depicts the phase distribution of the optimal weights. The progressive phase shift across the antenna elements ensures constructive interference in the desired direction, which is essential for accurate beam steering and the formation of a strong main beam.

 doi:10.20944/preprints202605.1202.v1

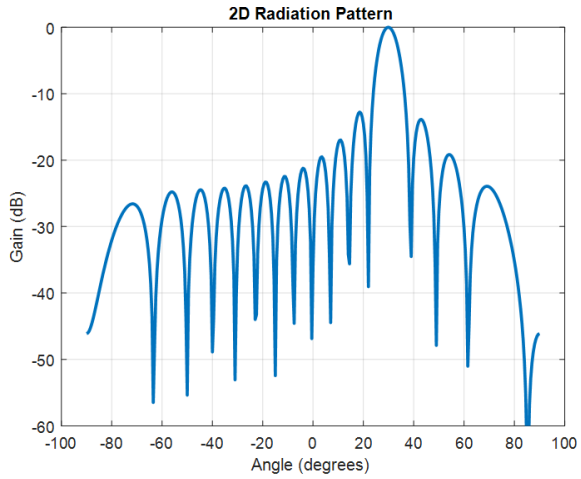

Figure 14. Normalized array factor (in dB), illustrating the radiation pattern and the direction of the main lobe.

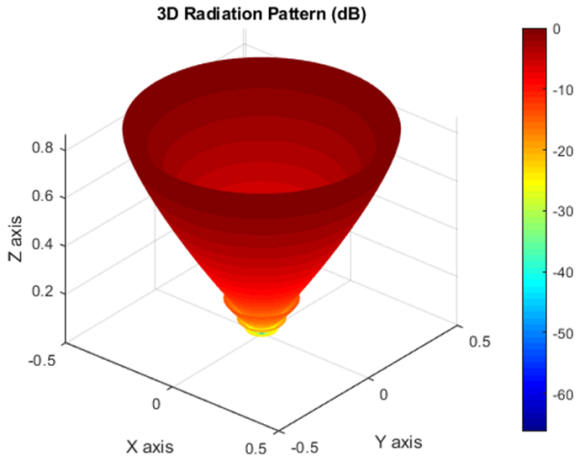

Figure 15. Radiation pattern in polar coordinates, showing the spatial distribution of the radiated energy.

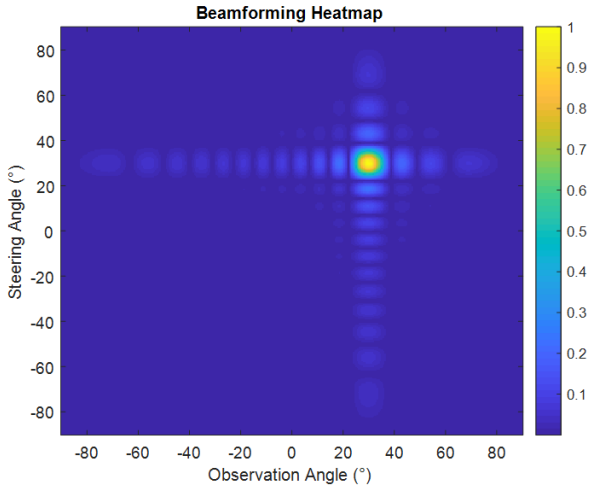

Figure 16. Magnitude of the optimal beamforming weights applied to the antenna array elements.

 doi:10.20944/preprints202605.1202.v1

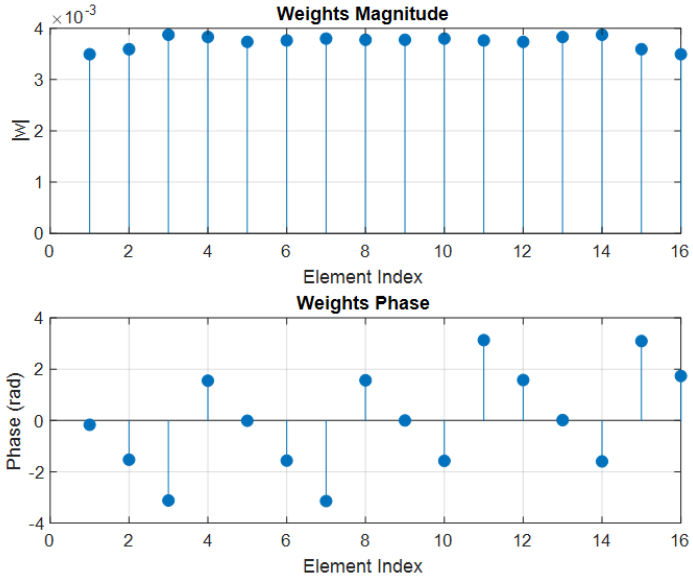

Figure 17. Phase distribution of the optimal weights used for beam steering.

Figure 18 compares the proposed beamforming technique with the conventional method. The proposed approach achieves lower side lobe levels and improved beam focusing, demonstrating superior performance in terms of radiation control and interference mitigation.

Figure 19 shows the beamforming heatmap over a range of steering angles. The results indicate that the proposed method maintains a consistent and stable beam response across multiple directions, highlighting its robustness and adaptability.

Figure 20 presents the three-dimensional radiation pattern of the antenna array. This figure provides a complete spatial visualization of the radiated energy, confirming high directivity and efficient energy concentration in the desired direction. The results validate the effectiveness of the proposed beamforming strategy for advanced wireless and radar applications.

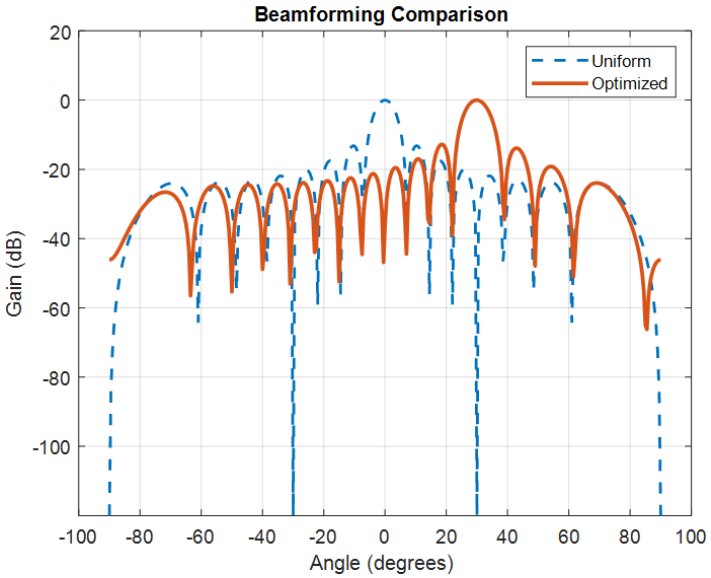

Figure 18. Performance comparison between the proposed beamforming method and the conventional approach.

 doi:10.20944/preprints202605.1202.v1

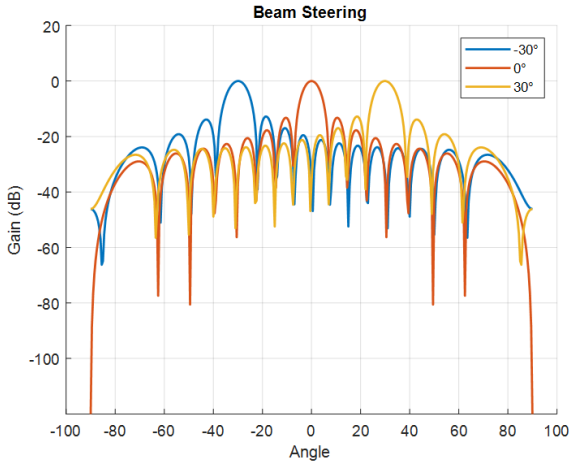

Figure 19. Beamforming heatmap showing the array response over multiple steering angles.

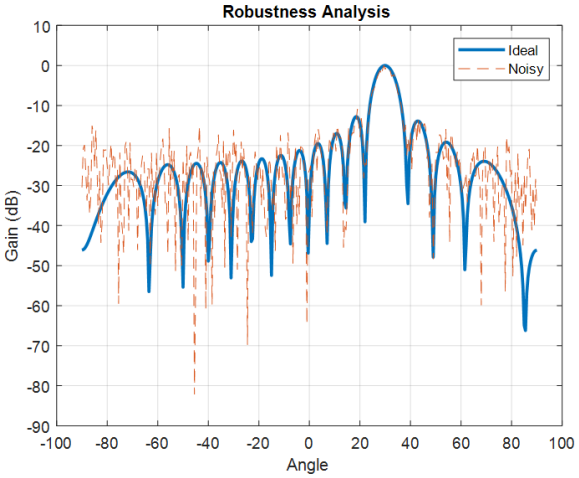

Figure 20. Three-dimensional radiation pattern (in dB), illustrating the spatial radiation characteristics of the antenna array.

4. Conclusions

This paper proposed a novel optimal control-based beamforming framework for phased antenna arrays, targeting applications in 5G wireless communications and radar systems. The beamforming problem was formulated as a discrete-time optimal control problem using a state-space representation, where a quadratic cost function was introduced to balance radiation pattern accuracy and excitation power.

The Linear Quadratic Regulator (LQR) approach was employed to compute the optimal excitation weights by solving the discrete-time algebraic Riccati equation. This method enables precise control of the radiation pattern while ensuring efficient power utilization and improved robustness compared to conventional techniques.

Simulation results demonstrated that the proposed method significantly enhances beamforming performance, achieving lower sidelobe levels, improved main lobe directivity, and accurate beam steering. In addition, the proposed framework exhibits strong potential for real-time implementation, particularly on FPGA-based and embedded platforms.

Future work will focus on extending the proposed approach to more complex scenarios, including planar and massive MIMO antenna arrays, as well as incorporating hardware constraints and experimental validation in real-world systems.

 doi:10.20944/preprints202605.1202.v1

Author Contributions: Conceptualization, M.T., Z.H., and A.G.; methodology, M.T., Z.H., and A.G.; software, M.T. and M.G.; validation, S.G. and A.G.; formal analysis, M.T., Z.H., and M.G.; investigation, M.T.; resources, S.G. and A.G.; data curation, M.T.; writing—original draft preparation, M.T.; writing—review and editing, Z.H., M.G., S.G., and A.G.; visualization, M.T.; supervision, A.G. and Z.H.; project administration, A.G.; All authors have read and agreed to the published version of the manuscript.

Funding: This research received no external funding.

Data Availability Statement: The data supporting the findings of this study are available from the corresponding author upon reasonable request.

Acknowledgments: The authors would like to thank the Laboratory of Microwave Electronics, Faculty of Sciences of Tunis, University of Tunis El Manar, Tunisia, for their support and collaboration. The authors also acknowledge the valuable contributions of all colleagues involved in discussions related to this work.

Conflicts of Interest: The authors declare no conflict of interest.

Abbreviations

The following abbreviations are used in this manuscript:

AF	Array Factor
LQR	Linear Quadratic Regulator
DARE	Discrete-Time Algebraic Riccati Equation
LMS	Least Mean Squares
RLS	Recursive Least Squares
MVDR	Minimum Variance Distortionless Response
PSO	Particle Swarm Optimization
GA	Genetic Algorithm
SOCP	Second-Order Cone Programming
ULA	Uniform Linear Array
FPGA	Field-Programmable Gate Array
DSP	Digital Signal Processing
MIMO	Multiple-Input Multiple-Output
SLL	Side Lobe Level
SNR	Signal-to-Noise Ratio
AI	Artificial Intelligence
ACO	Ant Colony Optimization
DE	Differential Evolution
5G	Fifth Generation Wireless Communication

References

1. A. Kouki, R. Kheder, W. Amara, R. Ghayoula, L. Latrach, L. Ben Ayed, and J. Fattahi, “Multi-Beam Antenna Array Synthesis Using the Fourier Method for Reliable 5G Applications,” Proc. 18th Int. Conf. on Electronics, Computers and Artificial Intelligence (ECAI), Pitesti, Romania, 26 June 2025, Paper No. 3228.
2. A. Kouki, R. Kheder, R. Ghayoula, I. El Gmati, L. Latrach, W. Amara, L. Ben Ayed, and J. Fattahi, “Phased Antenna-Array Synthesis Using the Fourier Method for Reliable 5G Applications,” MDPI Telecom, vol. 6, no. 2, 2025.
DOI: 10.3390/telecom6020037
3. R. Khedher, R. Ghayoula, A. Smida, I. El Gmati, L. Latrach, W. Amara, A. Hammami, J. Fattahi, and M. I. Waly, “Enhancing Beamforming Efficiency Utilizing Taguchi Optimization and Neural Network Acceleration,” MDPI Telecom, 2024, pp. 451–475.
https://www.mdpi.com/2673-4001/5/2/23
4. W. Amara, R. Kheder, R. Ghayoula, I. El Gmati, A. Smida, J. Fattahi, and L. Latrach, “Taguchi Method-Based Synthesis of a Circular Antenna Array for Enhanced IoT Applications,” MDPI Telecom, 2025, 6(1), 7.
https://www.mdpi.com/2673-4001/6/1/7

 doi:10.20944/preprints202605.1202.v1

5. W. Amara, R. Ghayoula, A. Hammami, A. Smida, I. El Gmati, and J. Fattahi, "Phased Array Antenna Controlled by FPGA-ARM Cortex-M Processor," Advanced Electromagnetics Journal, vol. 12, no. 3, August 2023, pp. 61–68.
6. R. Ghayoula, W. Amara, I. El Gmati, A. Smida, and J. Fattahi, "An Efficient FPGA Implementation of MUSIC Processor Using Cyclic Jacobi Method: LiDAR Applications," MDPI Applied Sciences, 2022, 12, 9726; https://www.mdpi.com/2076-3417/12/19/9726
7. H. L. Van Trees, *Optimum Array Processing*, Wiley, 2002.
8. L. C. Godara, "Application of antenna arrays to mobile communications, Part II: Beam-forming and direction-of-arrival considerations," Proc. IEEE, vol. 85, no. 8, pp. 1195–1245, 1997.
9. S. Haykin, *Adaptive Filter Theory*, 4th ed., Prentice Hall, 2002.
10. S. Boyd and L. Vandenberghe, *Convex Optimization*, Cambridge Univ. Press, 2004.
11. H. Zhu, X. Chen, and Y. Li, "Beamforming techniques for massive MIMO systems in 5G: Overview, classification, and trends," IEEE Commun. Surveys Tuts., vol. 21, no. 2, pp. 1249–1275, 2019.
12. R. S. Elliott, *Antenna Theory and Design*, Wiley, 2003.
13. C. L. Dolph, "A Current Distribution for Broadside Arrays Which Optimizes the Relationship Between Beam Width and Side-Lobe Level," Proc. IRE, vol. 34, no. 6, pp. 335–348, 1946.
14. T. T. Taylor, "Design of line-source antennas for narrow beamwidth and low side lobes," IRE Trans. Antennas Propag., vol. 3, no. 1, pp. 16–28, Jan. 1955.
15. R. L. Haupt, "Genetic algorithm in antenna design," IEEE Antennas Propag. Mag., vol. 37, no. 2, pp. 7–15, 1995.
16. W. L. Stutzman and G. A. Thiele, *Antenna Theory and Design*, Wiley, 2012.
17. D. Malioutov, M. Cetin, and A. S. Willsky, "A sparse signal reconstruction perspective for source localization with sensor arrays," IEEE Trans. Signal Process., 2005.
18. J. Kennedy and R. Eberhart, "Particle swarm optimization," in Proc. IEEE Int. Conf. Neural Networks, 1995, pp. 1942–1948.
19. R. Storn and K. Price, "Differential evolution–a simple and efficient heuristic for global optimization over continuous spaces," J. Global Optim., 1997.
20. X. S. Yang, "Firefly algorithms for multimodal optimization," 2009.
21. M. Dorigo and L. M. Gambardella, "Ant colony system: a cooperative learning approach to the traveling salesman problem," IEEE Trans. Evol. Comput., 1997.
22. E. J. Candès, J. Romberg, and T. Tao, "Robust uncertainty principles: Exact signal reconstruction from highly incomplete frequency information," IEEE Trans. Inf. Theory, 2006.
23. Y. Zhu et al., "Deep learning for beamforming in wireless communications," IEEE Commun. Surveys Tuts., 2019.
24. A. Vaswani et al., "Attention is all you need," in Advances in Neural Information Processing Systems (NeurIPS), 2017.
25. Y. Li, "A survey of reinforcement learning algorithms," 2013.
26. R. F. Stengel, *Optimal Control and Estimation*, Dover Publications, 1994.
27. D. Li and Y. Zhang, "Linear Quadratic Regulator (LQR) Design for Discrete-Time Systems," Int. J. Control Autom., vol. 9, no. 5, pp. 123–134, 2016.
28. X. Wang, Y. Liu, and Z. Zhang, "Optimal Beamforming for Radar and Communication Systems Based on Control Theory," IEEE Access, vol. 8, pp. 145123–145135, 2020.
29. Y. Liu, X. Wang, and Z. Zhang, "Adaptive Beamforming Based on Optimal Control Theory for Antenna Arrays," IEEE Trans. Antennas Propag., vol. 69, no. 10, pp. 6723–6735, Oct. 2021.